Evaluation of Solvent Effects in Isotropic and Anisotropic Dielectrics and in Ionic Solutions with a Unified Integral Equation Method: Theoretical Bases, Computational Implementation, and Numerical Applications

B. Mennucci,[†] E. Cancès,[‡] and J. Tomasi*[,†]

Dipartimento di Chimica e Chimica Industriale, Università di Pisa, via Risorgimento 35, 56126 Pisa, Italy, and CERMICS, Ecole Nationale des Ponts et Chaussées, 6 & 8 Avenue Blaise Pascal, Cité Descartes, 77455 Champs-sur-Marne Cedex 2, France

Received: June 16, 1997; In Final Form: September 12, 1997[⊗]

We present the full implementation of the integral equation formalism (IEF) we have recently formulated to treat solvent effects. The method exploits a single common approach for dielectrics of very different nature: standard isotropic liquids, intrinsically anisotropic media like liquid crystals, and ionic solutions. We report here an analysis of its both formal and technical details as well as some numerical applications addressed to state the achieved generalization to all kinds of molecular solutes and to show the equally reliable performances in treating such different environmental systems. In particular, we report, for isotropic liquids, data of solvation free energies and static (hyper)polarizabilities of various molecular solutes in water, for anisotropic dielectrics, a study of an S_N2 reaction, and finally, for ionic solution, a study of some structural aspects of ion pairing.

1. Introduction

Theoretical estimations of environmental effects of both properties and behavior of molecules in solution are performed according to a large variety of methods, which, however, can be classified according to two basically different strategies.

In the first, we collect supermolecule calculations and computer simulations.[1,2] Even if the philosophy of the two approaches is quite different, in both cases, a detailed description of the disposition and structure of molecules composing the liquid system is searched.

The second strategy, almost complementary to the first, collects methods in which a target subsystem, the "solute", eventually supplemented by a few nearby solvent molecules, is described at the microscopic level, while the secondary subsystem ("the solvent") is modeled as an infinite macroscopic continuum medium having suitable properties.

Nowadays, there are several approaches to be classified in this second domain.[3] Some among them belong to the category of semiempirical methods and some play a role in the study of complex solutes (e.g. molecules of biological interest). Other retain the formalism of the *in vacuo ab initio* molecular calculations, including in the Hamiltonian, and in the corresponding Schrödinger equation, an explicit expression of the solute−solvent potential. The latter approach, known with the name "effective Hamiltonian method", represents a very powerful quantum-mechanical (QM) treatment of the solvation problem and will be exploited in the present paper.

Here, we do not intend to develop a detailed and complete procedure to treat environmental effects, but rather to discuss some methodological and computational aspects of a method we have recently implemented to calculate the electrostatic interaction between a continuous polarizable medium and the solute (as "solute" one may also consider a solvation cluster).[4,5]

The electrostatic problem of a charge distribution embedded in a cavity surrounded by a continuum dielectric strongly depends on the macroscopic structural characteristics of the dielectric itself. In other words, the derivation of the basic theoretical background cannot be made without defining which kind of system we are taking into account; within the continuum framework, in which a simplified expression of the averaged distribution function of the solvent molecules is usually exploited, this preliminary classification can be limited to the form of the dielectric constant.

Limiting our attention to homogeneous solutions, we can define the following items: (1) homogeneous isotropic dielectrics, characterized by a constant scalar permittivity, ϵ; (2) homogeneous anisotropic dielectrics, characterized by a constant tensorial permittivity, $\boldsymbol{\epsilon}$.

In this basic classification, the standard definition of an infinitely dilute solution is implicitly assumed; actually we can find many interesting solute−solvent systems going beyond this approximation. A surely important, and hence largely studied, example is given by salt solutions in which the dissolved electrolyte charges are free to move in the surrounding medium.

At the best of our knowledge, no QM method developed until now allows to treat in a single approach dielectrics of such different nature, and/or so complex systems. On the contrary, in the present work, we shall show that the procedure we have implemented, called IEF (integral equation formalism), allows to reach a unified analytical solution of the corresponding electrostatic problem for all the quoted systems (namely, one or more solutes either in a common isotropic solvent, in an anisotropic dielectric, like liquid crystals and solid matrices, or in an ionic solution); this method can be thus considered as the first example giving equally reliable results for such different physical situations, all with the same theoretical approach, namely an integral equation formalism. A brief theoretical description of the way this can be achieved will be given below, as well as some numerical applications.

Just for completeness' sake, we recall that a full treatment of the medium effects should go beyond the homogeneous limit applying to all the systems quoted above, and take into account an inhomogeneous dielectric, characterized for example by a position dependent permittivity, $\epsilon(\vec{r})$. At the moment, this

* Corresponding author. Phone: 39.50.918244. Fax: 39.50.502270. Email: tomasi@dcci.unipi.it.
[†] Università di Pisa.
[‡] Ecole Nationale des Ponts et Chaussées.
[⊗] Abstract published in *Advance ACS Abstracts,* November 1, 1997.

S1089-5647(97)01959-7 CCC: $14.00

complex case is still open, even if our research on this field is active and interesting ideas have been already formulated.

2. Effective Hamiltonian and the Free Energy

In the effective Hamiltonian method the solvent S is represented by a homogeneous continuum medium which is polarized by the solute M placed in a cavity built in the bulk of the dielectric. The solute−solvent interactions are described in terms of a solvent reaction field.

In the QM version of the method the solute molecule is studied quantum mechanically and the interactions with the solvent are taken into account through an interaction potential $\hat{V}_R$ which acts as a perturbation on the solute Hamiltonian:

$$\hat{H}^0\psi^0 = E^0\psi^0 \quad \text{in vacuo}$$

$$[\hat{H}^0 + \hat{V}_R]\,\psi = E\psi \quad \text{in solution} \tag{1}$$

where $\hat{H}^0$ is the Hamiltonian of the solute in vacuo, ψ^0 and ψ are the solute wave functions in vacuo and in solution, respectively.

In eq 1 the Born−Oppenheimer (BO) approximation is employed. This means a standard partition of the Hamiltonian into an electronic and a nuclear part, as well as the factorization of the wave function into an electronic and a nuclear component. In this approximation eq 1 refers to the electronic wave function with the electronic Hamiltonian dependent on the coordinates of the N_{el} electrons, and, parametrically, on the coordinates of the N_{nuc} nuclei.

The definition of the interaction potential $\hat{V}_R$ implies the knowledge of a thermally averaged distribution function of the solvent molecules. The basic energetic outcome of the model is thus a quantity having the status of a free energy; the formal relationship between this free energy G and the energy E of eq 1 can be derived in the following way.

A helpful strategy is to extract the contribution of the interaction potential $\hat{V}_R$ to be added to the Hamiltonian of the solute which explicitly depends on the solute electronic wave function, so that

$$\hat{V}_R = \hat{V}'_R(\Phi) + \hat{V}''_R \tag{2}$$

where the term $\hat{V}'_R(\Phi)$ has the form $\hat{V}'_R(\Phi) = \hat{A}(\Phi\Phi^*)$, with $\hat{A}$ given by a suitable integral operator.

Within this picture it is easy to show[6] that the variational solution of eq 1 requires the minimization of the functional

$$G(\Phi) = \langle\Phi|\hat{H}^0 + \hat{V}''_R + {}^1/_2\hat{V}'_R(\Phi)|\Phi\rangle \tag{3}$$

under the constraint $\langle\Phi|\Phi\rangle = 1$. The kernel of eq 3 differs from the operator in eq 1 as the wave function dependent component of $\hat{V}_R$ has been divided by 2. The factor $^1/_2$ has to be generalized to $1/(1 + q)$ when the dependence of the operator on the solute electronic charge distribution, ρ^e_M, goes as the power q, i.e., when we have $\hat{V}'_R(\Phi) = \hat{A}[(\Phi\Phi^*)^q]$; clearly, eq 3 is just the result of a linear dependence on ρ^e_M, or equivalently of a quadratic dependence on the wave function.

To completely define the total free energy of the system we have to choose the reference state (in our case it is given by noninteracting nuclei and electrons of M, supplemented by the unperturbed, i.e., unpolarized, pure liquid S) and take into account all the contributions not present in the interaction potential.

In the formalism we shall present in the following sections we exploit a simplified form of the interaction potential; $\hat{V}_R$ is reduced to its classical electrostatic component. In this approximation, all the other terms of steric and dispersion origin to be always considered in the definition of the total free energy[3] are not included in the QM evaluation of the solute wave function, but they are computed by resorting to separate calculations based on empirical parameters or other simplifying assumptions. Their contributions can be thus collected in a single term, indicated below as G_{nel} in order to stress its nonelectrostatic character, which will be not considered in the present paper. Within this picture the total free energy can be written as

$$G = \langle\psi|\hat{H}^0|\psi\rangle + \langle\psi|^1/_2\hat{V}'_R(\psi)|\psi\rangle + \langle\psi|\hat{V}''_R|\psi\rangle + {}^1/_2U_{NN} = V_{NN} + G_{nel} \tag{4}$$

where ψ is now the exact wave function and V_{NN} the nuclear repulsion energy of the solute M. The term U_{NN}, introduced here with factor $^1/_2$ in order to have a free energy, represents the interaction energy between solute nuclei and the solvent reaction field component generated by the nuclear part of the solute distribution (see next section for further details).

Note that the definition of G given in eq 4 does not contain contributions due to thermal motions of the molecules. On the contrary, in order to get the most complete definition of the free energy of solvation, we should supplement both the given definition of G in solution and of E^0 in vacuo with these entropic contributions. Actually, in computational practice, use is often made of a "reduced" solvation energy, $G-E^0$, in which the difference between the molecular motion contributions calculated in vacuo and in solution is neglected. The error caused by this approximation is generally quite limited.

Electrostatic Contribution. Once we have defined the system, a solute M in a cavity C surrounded by an infinite dielectric with a given function for the permittivity ϵ, the basic relation to be considered may be unified under a single formalism; namely, if we indicate with the subscripts e and i the regions outside and inside the cavity, respectively, we can write

$$L_iV = 4\pi\rho_M \quad \text{in } C$$

$$L_eV = 0 \quad \text{outside } C$$

$$[V] = \quad \text{on } \Sigma$$

$$[\partial_L V] = 0 \quad \text{on } \Sigma \tag{5}$$

where $L_i = -\Delta$, V is the electrostatic potential due to the presence of the charge distribution ρ_M located inside the cavity, and Σ is the cavity surface. The operator L_e has to be differently defined for each particular system we are considering; in particular:

$$L_eV = -\epsilon\Delta V \quad \text{for isotropic dielectrics}$$

$$L_eV = -\mathrm{div}(\boldsymbol{\epsilon}\cdot\nabla\Delta) \quad \text{for anisotropic dielectrics}$$

$$L_eV = -\epsilon\Delta V + \epsilon\kappa^2 V \quad \text{for ionic solutions}$$

The jump condition $[V] = 0$, means that the potential V is continuous across the interface Σ, i.e., $V_e - V_i = 0$ on Σ. The equality $[\partial_L V] = 0$ is a formal expression of the jump condition of the gradient of the potential; in the limit of a homogeneous isotropic system it takes the well-known form

$$\left(\frac{\partial V}{\partial n}\right)_{\mathrm{i}} - \epsilon\left(\frac{\partial V}{\partial n}\right)_{\mathrm{e}} = 0 \tag{6}$$

where n is the outward pointing unit vector perpendicular to the cavity and system (5) reduces to the basic Poisson equation.

In addition, it is easy to see that for ionic solutions the same system is nothing but the so-called linearized Poisson−Boltzmann (LPB) equation, where the constant κ accounts for the ion screening (its inverse is known as the Debye length), namely:

$$\kappa^2 = \frac{8\pi I F^2}{\epsilon_2 RT} \quad \text{with} \quad \frac{1}{2}\sum_i c_i z_i^2 \tag{7}$$

where I is the ionic strength, F the Faraday constant, ϵ_2 the dielectric constant of the medium, equal to its relative constant multiplied by the permittivity of vacuum, R the gas content, T the absolute temperature in K, c_i the concentration of the ith ionic species in moles per cubic meter, and z_i its charge in units of the elementary charge.

Here, it is worth recalling that the LPB equation is an approximation obtained by taking only the linear term in the Taylor expansion series of the hyperbolic sine function which appears in the more general Poisson−Boltzmann description. That is, the linearization of the PB equation is a result of the Debye−Huckel approximation applicable in the case of low potentials, a condition approached at low concentrations. For electrolytes of high-valence type and for electrolytes in media of low dielectric constant, the same approximation becomes not good.[7]

The solution of the general system (5) is quite a hard task.

Until now, the solutions found have been obtained by exploiting different approaches for each particular system.

Thus, in the case of isotropic dielectrics, the most diffused computational methods exploit an approach based on Green functions; their knowledge enables one to transform the first two equations in (5) into integral equations on the surface Σ that can be easily solved with standard numerical methods. In this framework, the solution of system (5) is given by the sum of two electrostatic potentials, one produced by ρ_{M} and the other due to a surface charge distribution σ, placed on the interface, arising from the polarization of the dielectric medium:

$$V(x) = V_{\mathrm{M}}(x) + V_\sigma(x) = \int_{R^3}\frac{\rho_{\mathrm{M}}(y)}{|x-y|}\,\mathrm{d}y + \int_\Sigma \frac{\sigma(s)}{|x-s|}\,\mathrm{d}s \tag{8}$$

where the integral on the first term is taken over the entire three-dimensional space.

On the contrary, for the two other systems, i.e., anisotropic dielectrics and ionic solutions, the methods used so far are based on three-dimensional techniques, like finite element or finite difference methods, much less effective than the integral equations formalism exploited above both in terms of numerical accuracy and computational costs.

As anticipated in the Introduction, the IEF method[4,5] we are presenting here is, to the best of our knowledge, the first example of a formalism which manages to treat all the different solvation systems listed above within a common integral equation-like approach. In other words, the same considerations given above for the isotropic model which lead to definition of eq 8 are still valid also for the other two more complex systems. The only but nontrivial problem consists in the calculation of the screening, or apparent (from which it derives the acronym, ASC, defining the class of methods the present one belongs to), surface charge density $\sigma(s)$ in the various systems.

The strategy followed in the IEF method is based on the use of specific operators, well-known in the theory of integral equations,[8] but not so diffused in the theoretical treatment of chemical problems. We do not report here their formal derivations, as this would be too long and almost out of the scope of this presentation, but we limit ourselves to write the final expressions; the full mathematical treatment can be found in the still unpublished ref 4, but many useful details are also present in the recently published ref 5.

By denoting with G_{i} and G_{e} the standard Green functions of the operators L_{i}, and L_{e} introduced in eq 5, respectively:

$$G_{\mathrm{i}}(x,y) = 1/|x-y| \qquad \text{if } x \in C \tag{9}$$

$$G_{\mathrm{e}}(x,y) = \begin{cases} (\epsilon|x-y|)^{-1} & \text{(isotropic)} \\ (\sqrt{\det\epsilon})^{-1}[(\epsilon^{-1}(x-y))\cdot(x-y)]^{-1/2} & \text{(anisotropic)} \\ \exp(-\kappa|x-y|)(\epsilon|x-y|)^{-1} & \text{(ionic solution)} \end{cases} \qquad \text{if } x \notin C \tag{10}$$

where C indicates the cavity; we can write the operators to be used as follows:

$$\begin{aligned} (S_{\mathrm{i}}\cdot\mathrm{u})(x) &= \int_\Sigma G_{\mathrm{i}}(x,y)u(y)\,\mathrm{d}y \\ (D_{\mathrm{i}}\cdot u)(x) &= \int_\Sigma \partial_y G_{\mathrm{i}}(x,y)u(y)\,\mathrm{d}y \\ (D_{\mathrm{i}}^{*}u)(x) &= \int_\Sigma \partial_x G_{\mathrm{i}}(x,y)u(y)\,\mathrm{d}y \end{aligned} \tag{11}$$

where u is a function defined on the the cavity boundary Σ, and x, $y \in \in$. In eq 11 we have exploited the contracted formalism $\partial_y G_{\mathrm{i}}(x,y) = \nabla_y G_{\mathrm{i}}(x,y)\cdot n(y)$, $\partial_x G_{\mathrm{i}}(x,y) = \nabla_x G_{\mathrm{i}}(x,y)\cdot n(x)$, being n the outward pointing normal. We also recall that the operator S_{i} is self-adjoint, and $D_{\mathrm{i}}^{*}$is the adjoint of D_{i}.

In a parallel way, we can define two other operators, S_{e} and D_{e}, by replacing G_{i} of eq 11 with the corresponding function G_{e} defined in the outer space. In this case the derivative operator means $\partial_y G_{\mathrm{e}}(x,y) = (\epsilon\cdot\nabla_y G_{\mathrm{e}}(x,y))\cdot n(y)$, where the dielectric matrix reduces to the scalar dielectric constant for both isotropic media and ionic solutions.

Here we do not report the formal derivation that, exploiting specific characteristics of these operators, leads to the definition of the surface charge σ, as it is too technical (the interested reader can find it in ref 4), but we only say the latter is the unique solution to the equation:

$$A\cdot\sigma = -g \tag{12}$$

where

$$\begin{aligned} A &= \left(\frac{I}{2} - D_{\mathrm{e}}\right)S_{\mathrm{i}} + S_{\mathrm{e}}\left(\frac{I}{2} + D_{\mathrm{i}}^{*}\right) \\ g &= \left(\frac{I}{2} - D_{\mathrm{e}}\right)V - S_{\mathrm{e}}E_{\mathrm{n}} \end{aligned} \tag{13}$$

V and E_{n} being the potential and the normal component of the electric field created by ρ_{M}, respectively, and I the unit operator.

At this point it is worth making a brief digression to show a very important aspect of this formalism.

In the Introduction we have said that the most diffused ACS methods, addressed and limited to treat isotropic dielectrics, exploit a Green function formalism; in stating that we were implicitly referring to a particular computational method, i.e., the PCM, which from its first appearance in 1981[9] has spread out because of its adaptability and accuracy . The evolution of

PCM during the years has made it one of the most powerful QM solvation methods;[3] indeed, the IEF method also, for its computational implementation, exploits many features originally derived for standard PCM.

The formal derivation of PCM method has been reported in several papers,[3,9,10] and we do not repeat here all the details; suffice it to say that the ASC distribution σ of eq 8 is discretized in a finite set of apparent charge by exploiting a partition of the cavity surface in T small elements (called tesserae) of known area a_k. The electrostatic formulas giving these point charges may be expressed as a set of linear equations, whose matrix form is the following:

$$\mathbf{D}\mathbf{A}^{-1}\mathbf{q} = -\mathbf{E}_n \tag{14}$$

where $\mathbf{q}$ is the column matrix collecting the charges, $\mathbf{D}$ a square matrix, with elements determined by the value of the normal components of the field the apparent charges induce on each other (i.e., the solvent reaction field), and $\mathbf{A}$ a square diagonal matrix, of same dimension as $\mathbf{D}$, with elements equal to the tesserae's areas: $A_{kk} = a_k$. The column matrix $\mathbf{E}_n$ contains the solute electrostatic field component perpendicular to the cavity surface at each tessera.

Very recently, the PCM has been complemented with a new option which allows the use of an other ASC method, called COSMO, still remaining in the QM framework of standard PCM.[11] This new option has been implemented on the basis of the original COSMO elaboration given by Klamt and Schüürmann,[12] but without using their computer codes.

COSMO is based on a screening conductor theory. In our framework of a solute M placed in a cavity inside the medium, now represented by a conductor, the boundary condition to be fulfilled is that the total potential V cancels out on the surface Σ of the cavity. By following the strategy already used in the PCM method, from this condition we can derive the basic system giving the COSMO apparent charges in the following matrix formalism:

$$\mathbf{B}\mathbf{A}^{-1}\mathbf{q} = -\frac{\epsilon - 1}{\epsilon}\mathbf{V} \tag{15}$$

where the column matrix $\mathbf{V}$, of dimension equal to the number T of the tesserae, contains the solute electrostatic potential on each tessera, and the elements of $(T \times T)$ matrix $\mathbf{B}$ are the reaction field potential the apparent charges exerts on themselves.

The factor $(\epsilon - 1)/\epsilon$ of eq 15 has been introduced a posteriori in order to allow the passage from the real conductor, with $\epsilon = \infty$, for which the COSMO equation is analytically derived, to a solvent with dielectric constant ϵ.

The brief summary given above, for the main characteristics of these two very popular ASC methods allows us to show an interesting aspect which is specific to IEF formalism, namely that it contains standard PCM as a specific case of the isotropic system and goes to COSMO in the limit of infinite dielectric permittivity. In the following we report a very concise derivation of both these points.

In the case of an isotropic dielectric, for which we have $S_e = S_i/\epsilon$, and $D_e = D_i$, eq 12 becomes

$$S_i\left[\left(\frac{I}{2} - D_i^*\right) + \frac{1}{\epsilon}\left(\frac{I}{2} + D_i^*\right)\right]\sigma = -\frac{\epsilon - 1}{\epsilon}S_i E_n \tag{16}$$

where we have exploited the formal relations $D_i S_i = S_i D_i^*$ and $(I/2 - D_i)V - S_i E_n = 0$.[4] After multiplication by $\epsilon/(\epsilon - 1)S_i^{-1}$, we obtain

$$\left(\frac{\epsilon + 1I}{\epsilon - 12} - D_i^*\right)\sigma = -E_n \tag{17}$$

which is the operator-like form of the basic matrix equation defining the apparent charges in the standard PCM procedure.

In a similar way, if we rewrite eq 12 by exploiting the same relations used to get eq 16, but this time in terms of the potential V instead of the normal field, we obtain

$$\left[\left(\frac{I}{2} - D_i\right) + \frac{1}{\epsilon}\left(\frac{I}{2} + D_i\right)\right]S_i\sigma = -\frac{\epsilon - 1}{\epsilon}\left(\frac{I}{2} - D_i\right)V \tag{18}$$

If then we assume that $\epsilon \rightarrow \infty$, i.e., we consider the conductor limit case, the second term between square brackets disappears and the ratio $(\epsilon - 1)/\epsilon$ becomes one, hence after multiplication by $(I/2 - D_i)^{-1}$, we obtain

$$S_i\sigma = -V \tag{19}$$

which is the operator-like form of the matrix equation (15) obtained above for the standard COSO procedure.

Let us now go back to technical aspects related to the computational implementation of the IEF method.

As for standard PCM procedure, also for IEF we exploit a tessellation of the cavity surface into T tesserae, and approximate the charge density σ by a piecewise constant function (i.e., a function constant on each tessera). In this approximation, eq 12 amounts to a linear system of order T denoted

$$\mathbf{C}\mathbf{A}^{-1}\mathbf{q} = -\mathbf{g} \tag{20}$$

where $\mathbf{q}$ is the column vector containing the apparent charges on the single tesserae, $\mathbf{C}$ a $(T \times T)$ matrix, $\mathbf{A}^{-1}$ the inverse of the usual diagonal matrix $\mathbf{A}$ of tesserae areas, and $\mathbf{g}$ a column vector depending on the solute charge distribution ρ_M.

Starting from the operator analog of eq 20, we easily obtain

$$\mathbf{C} = (\mathbf{A}/2 - \mathbf{D}_e)\mathbf{A}^{-1}\mathbf{S}_i + \mathbf{S}_e\mathbf{A}^{-1}(\mathbf{A}/2 + \mathbf{D}_i^*)$$

$$\mathbf{g} = (\mathbf{A}/2 - \mathbf{D}_e)\mathbf{V} - \mathbf{S}_e\mathbf{E}_n \tag{21}$$

Equation 21 clearly shows that in the IEF method, the working matrices $\mathbf{C}$ and $\mathbf{g}$ have a by far more complex form than the analogs defined for both PCM and COSMO; however, all the quantities appearing in eq 21 can be related to the potential and electric field-like matrices already defined for the other two ASC methods. In particular, $\mathbf{D}_x$ square matrices can be associated to the PCM matrix $\mathbf{D}$, whose elements give the normal components of the field the apparent charges induce on each other (i.e., the solvent reaction field), while $\mathbf{S}_x$ matrices to the parallel COSMO matrix $\mathbf{B}$, collecting the reaction potential the same apparent charges exert on themselves. In a parallel way, in the definition of $\mathbf{g}$ we can recognize the already defined column matrices $\mathbf{E}_n$ and $\mathbf{V}$ containing the solute electrostatic field component perpendicular to the cavity surface and the solute electrostatic potential, both computed at each tessera, respectively.

This correspondence with well-known quantities allows us to define the elements of each matrix, as follows. For all $1 < k \neq k' \leq T$, we have

$$S_i^{kk'} = a_k a_{k'}/|s_k - s_{k'}|$$

$$D_i^{kk'} = a_k a_{k'}[(s_k - s_{k'})\cdot n(s_{k'})/|s_k - s_{k'}|^3] \tag{22}$$

where vector s_k indicates the "representative" point of tessera k at which the charge q_k is placed.

Regarding the correspondent diagonal terms, when the tessera is placed on a sphere of radius R, it can be shown that $D_i^{kk} = -S_i^{kk}/(2R)$, where $S_i^{kk} = 1.07a_k\sqrt{4\pi a_k}$. The latter term, based on the analysis given by Klamt and Schüürmann in their space of presentation of the already quoted COSMO method,[12] is derived for the simple model of a homogeneously charged spherical surface partitioned into equivalent segments by the vertices of a regular polyhedron inscribed in it.

The definition of the parallel $\mathbf{S}_e$ and $\mathbf{D}_e$ matrices needs further considerations, these being the quantities which depend on the specific system under scrutiny.

In the simplest isotropic case they are computed applying the relations $\mathbf{S}_e = \mathbf{S}_i/\epsilon$, and $\mathbf{D}_e = \mathbf{D}_i$, as one can easily see from the corresponding relation in the G_i and G_e functions (see eqs 9−10). In both the remaining systems we cannot exploit such simple relations no longer valid, but we have to derive the specific expressions of $\mathbf{S}_e$ and $\mathbf{D}_e$ from the definition of the related operators. That is, for the off-diagonal elements we obtain

$$S_e^{kk'} = \begin{cases} a_k a_{k'} (\sqrt{\det \epsilon})^{-1}[(\epsilon^{-1}(s_{kk'}))\cdot s_{kk'}]^{-1/2} & \text{(anisotropic)} \\ a_k a_{k'} \exp(-\kappa|s_{kk'}|)(\epsilon|s_{kk'}|)^{-1} & \text{(ionic solutions)} \end{cases} \quad (23)$$

$$D_e^{kk'} = \begin{cases} a_k a_{k'} (\sqrt{\det \epsilon})^{-1}[s_{kk'}\cdot n(s_{k'})][(\epsilon^{-1}(s_{kk'}))\cdot s_{kk'}]^{-3/2} & \text{(anisotropic)} \\ a_k a_{k'} \exp(-\kappa|s_{kk'}|)(1+\kappa|s_{kk'}|)[s_{kk'}\cdot n(s_{k'})]|s_{kk'}|^{-3} & \text{(ionic solutions)} \end{cases} \quad (24)$$

where we have exploited a contracted formalism for the vector notation, namely $s_{kk'} = s_k - s_{k'}$.

Regarding the diagonal elements, we cannot derive simple expressions as done for the corresponding (i) matrices, but we have to use standard numerical interaction techniques; namely, by exploiting the same approximation of a piecewise constant charge density, the expression to be computed reduces to

$$I = a_k \int_k G(s_k,s)\, \mathrm{d}s \quad (25)$$

where G is either the kernel G_e or ∂G_e. Using polar coordinates centered at s_k, the integral of eq 25 reduces to the integral of a regular function over the boundary of the tessera and is easily evaluated in a numerical way with a one-dimensional Gauss rule.

Both the definitions of the matrix elements given in eqs 22−24 and, of the related diagonal analogs, have implied a great improvement with respect to what is reported in the two already quoted papers on the original version of IEF.[4,5] In the latter in fact, we stated that the cavity tessellation exploited in standard PCM, known as GEPOL procedure,[13] did not fit for the IEF method, as it seemed to lead to numerical instabilities. For this reason, we preferred to implement a different tessellation procedure which exploited meridian and parallel-like divisions. On the contrary, the implementation of the definitions above, performed after the submission of the two articles, have clearly shown that GEPOL tessellation can be exploited also for the IEF method without any difference with respect to PCM. As a very important consequence, the limitations to simple cavities characterizing the original versions have been completely overcome, and the IEF method has now exactly the same general applicability to molecular solutes of any shape as standard PCM.

At this point, the whole electrostatic problem is unequivocally determined and the strategy to be followed almost completely identified.

As we have said above, many computational features exploited by IEF derive from the PCM program; in particular, the QM procedure used to get the solute wave function and the solvation free energy is completely equivalent to that formulated for standard PCM, and it is repeated here to give a self-consistent exposition of the IEF method.

If we exploit the partition of the potential $\mathbf{V}$, and the field $\mathbf{E}_n$ matrices defining $\mathbf{g}$, into the electronic and nuclear components, we obtain a parallel partition into electrons and nuclei-induced apparent charges:

$$\mathbf{q} = \mathbf{q}^e + \mathbf{q}^N = -\mathbf{A}\mathbf{C}^{-1}(\mathbf{g}^e + \mathbf{g}^N) \quad (26)$$

In this framework also the solute−solvent interaction energy may be divided into four different contributions:

$$U_{MS} = \int\int \frac{\rho(x)\sigma(s)}{|x-s|}\, \mathrm{d}x\, \mathrm{d}s = U_{ee} + U_{eN} + U_{Ne} + U_{NN} \quad (27)$$

where the first subscript refers to the component of the solute charge and the second to that of the ASC.

In order to go inside the effective Hamiltonian procedure exploited in this method, it is useful to limit the quantum calculation to the Hartree−Fock approximation of a closed-shell molecule, in which each molecular orbital is expressed as a linear combination over a finite atomic orbital basis set, here represented by the column matrix χ. The extension to open-shell cases is immediate.

In this approximation the first three contributions to the interaction enenergy of eq 27 (the last term U_{NN} is a constant dependent only on the positions and the charges of solute nuclei) can be expressed in terms of three matrices, $\mathbf{X}(\mathbf{P})$, $\mathbf{j}$, and $\mathbf{y}$, collecting solute−solvent interaction terms, so that:

$$\begin{aligned} U_{ee} &= \mathrm{tr}\, \mathbf{P}\mathbf{X}(\mathbf{P}) \\ U_{eN} &= \mathrm{tr}\, \mathbf{P}\mathbf{j} \\ U_{Ne} &= \mathrm{tr}\, \mathbf{P}\mathbf{y} \end{aligned} \quad (28)$$

where $\mathbf{P}$ is the solute one electron density matrix. In particular, $\mathbf{j}$ is the matrix collecting the interactions between each solute electronic elementary charge distribution $\chi_\mu\chi_\nu$ and the nuclei-induced apparent charges $\mathbf{q}^N$, $\mathbf{y}$ the matrix related to the interaction between solute nuclear charges and the electron-induced apparent charges $\mathbf{q}^e$, and $\mathbf{X}(\mathbf{P})$ the matrix defining the interactions between solute electrons and the apparent charges $\mathbf{q}^e$.

The expression for the corresponding electrostatic component of the free energy can be easily written as

$$\begin{aligned} G &= \mathrm{tr}\, \mathbf{P}\,[\mathbf{h} + {}^1/_2(\mathbf{j}+\mathbf{y})] + {}^1/_2\, \mathrm{tr}\, \mathbf{P}\,[\mathbf{G}(\mathbf{P}) + \mathbf{X}(\mathbf{P})] + [{}^1/_2 U_{NN} + V_{NN}] \\ &= \mathrm{tr}\, \mathbf{P}\mathbf{h}' + {}^1/_2\, \mathrm{tr}\, \mathrm{P}\mathrm{G}'(\mathbf{P}) + V'_{NN} \end{aligned} \quad (29)$$

where $\mathbf{h}$, $\mathbf{G}(\mathbf{P})$, and V_{NN} are the elements used in standard calculations in vacuo, collecting one electron integrals, two-electron integrals, and nuclear repulsion, respectively. Here, the prime on the matrices in the right-hand expression, which is formally identical to the of E^0 for the system in vacuo, is to stress that the corresponding term takes into account the contribution due to the solvent.

By combining the stationary condition $\delta G = 0$ for an arbitrary variation of the molecular orbital coefficients $\mathbf{C}$, with the

auxiliary conditions of orthonormality, one easily arrives at the following HF-like equation:

$$\mathbf{F}'\mathbf{C} = [\mathbf{h}' + \mathbf{G}'(\mathbf{P})]\mathbf{C} = \mathbf{S}\mathbf{C}\boldsymbol{\varepsilon} \tag{30}$$

where we have used the same meaning for the prime on the Fock matrix of the system in solution. Here, **S** and $\boldsymbol{\varepsilon}$ represent the standard overlap and one-electron orbital matrices, exactly as in vacuo. In order to avoid any misunderstanding we point out the fact that the symbols **S** and **C**, which are used here in their standard meaning as overlap and coefficient matrices, have been used in another meaning before (see eqs 20−21); however, we thank that the reader has managed to distinguish the proper meaning in each context without confusion.

Equation 30 can be solved with the same iterative procedure of the problem in vacuo; the only difference introduced by the presence of the continuum dielectric is that, at each SCF cycle, one has to simultaneously solve the standard quantum mechanical problem and the additional electrostatic problem of the evaluation of the interaction matrices, and hence of the apparent charges. The latter are obtained from eq 26 through a self-consistent technique which has to be nested to that determining the solute wave function; as a consequence, in each cycle, and a fortiori at the convergency, solute and solvent distribution charges are mutually equilibrated.

As a final technical note we add that the more complex form of the matrices comparing in the basic equation (20), with respect to the parallel ones exploited in PCM and COSMO (see eq 14 and 15, respectively), affects both the computational times and the required storage dimension of IEF method. In particular, in order to evaluate matrix **C** four matrices are needed: $\mathbf{S}_e$, $\mathbf{S}_i$, $\mathbf{D}_e$, and $\mathbf{D}_i$, or better its transpose $\mathbf{D}_i^*$(only in the isotropic case they reduce to two, thanks to the simple relations $\mathbf{S}_e = \mathbf{S}_i/\epsilon$ and $\mathbf{D}_e = \mathrm{D}_i$). Moreover, since the **g** matrix, which cannot be defined once but has to be recomputed at each SCF cycle, as it is dependent on the solute density matrix through the potential **V**, and the field $\mathbf{E}_n$ matrices, is given by a combination of different matrices, a supplementary memory occupation is needed; in other words the final number of matrices which, belong constant during the QM calculation, are computed once and then stored, or eventually written on disk and read when required, is 3 (i.e., $\mathbf{C}^{-1}$, $\mathbf{S}_e$, and $\mathbf{D}_e$) and not 1 as in PCM or COSMO. However, all these further computational requests have no great effect on the global performance of the IEF method, as the most time-consuming step, namely that of the inversion of matrix **C**, is exactly equivalent to the parallel one required for both PCM matrix **D** and COSMO matrix **B**, being dependent on the common dimension of the problem, i.e., the number of tesserae (namely, time $\approx T^3$). Numerical examples of CPU times for IEF and PCM methods will be given in the following section.

Before going into the numerical analysis it is worth making a brief digression on a very important aspect, common to all the ASC methods, namely the errors induced either by the use of an apparent surface charge distribution spread on the cavity embedding the solute, or by its discretization into point charges. Here, the evaluation of these errors will be used as a fundamental point to state the reliability of the IEF method, and as a comparative tool with other similar ASC methods.

3. Errors on the Total Apparent Charge

According to the Gauss theorem there is a simple relation between the solute charge Q_M^d and the integral of the corresponding apparent charge distribution σ^d, where the subscript d indicates the type of charge we are taking into account, i.e., total (T), nuclear (N), or electronic (e):

$$\int_\Sigma \sigma^d(s)\, ds = -\frac{\epsilon - 1}{\epsilon} Q_M^d \tag{31}$$

In general, this formal relation is no longer fulfilled when we introduce the discrete representation of the surface distribution charge in terms of a piecewise constant function defined on the surface tesserae; namely, rougher the way this approximation is performed (i.e., rougher is the tessellation procedure) greater the difference between the two quantities of eq 31.

Actually, when d = e the Gauss relation is not fulfilled also for another reason of physical, and not numerical, origin.[15,16] In the definition of σ^e, one assumes that the whole solute electronic distribution charge ρ_M^e is bounded within the cavity; however, in quantum mechanical calculations, this charge distribution has always tails spreading outside the cavity, whose magnitudes depend on the basis set used and, of course, the dimension of the cavity.

In all the above-quoted ASC methods (namely PCM, COSMO, and IEF), the two different errors (i.e., discretization and the tail errors) are easily quantified in terms of the difference between the theoretical and the computed value of the total apparent charge:

$$\Delta_\sigma^d = Q_\sigma^d(\mathrm{theo}) - Q_\sigma^d(\mathrm{comp}) \tag{32}$$

and some numerical corrections that, even if they do not eliminate the source of the errors, alleviate the consequences they have on the solute energy and wave function, can be eventually introduced. These corrections have been put under the form of a renormalization or the apparent point charges $\{q_k\}$ placed on the tesserae. Since the first paper on PCM, in which this problem was originally pointed out, many techniques of renormalization, also called compensation procedures, have been given:[9,10,18] the interested reader can find some examples and a quite detailed analysis of the performances of the various techniques in a paper of very recent submission.[17]

Here, we shall focus our attention on two specific procedures implemented in the most recent version of PCM; in the following they will be called N2-PCM and N4-PCM, respectively. For a better understanding it is worth recalling here the main characteristics and differences of these two procedures.

The strategy followed to define the N2 normalization procedure is based on the observation that $\mathbf{q}^N$ charges are affected by the discretization error only, which, in contrast to the tail error, is constant during the whole calculation. Thus, once the total nuclear apparent charge $Q_\sigma^N(\mathrm{comp})$, given by the sum of all the $\mathbf{q}^N$, is computed, the error we make on it can be definitely corrected by multiplying each charge by a constant factor, such that $f^N = Q_\sigma^N(\mathrm{theo})/Q_\sigma^N(\mathrm{comp})$. The same strategy is then applied to the complementary set of electronic apparent charges $\mathbf{q}^e$, even if here the parallel correction factor f^e has to be recomputed at each change of the solute wave function; the error on $Q_\sigma^e(\mathrm{comp})$ is in fact dependent on the solute electronic tails, besides the discretization, and cannot be constant during the SCF iteration procedure.

The fundamental limits of this easy and fast technique is that it does not allow to separate the two sources of errors, i.e., the numerical and the physical, and, more important, it cannot take into correct account eventual local effects due, for example, to a very asymmetric electronic charge distribution in the solute that leads to different amounts of escaped charge on the various region of the cavity.

In order to overcome all these limitations, quite recently a new procedure, here indicated as N4, has been formulated.[18] In

TABLE 1: Solvation Data and CPU Times of H_2CO, H_2CNH, and HNCO Obtained with Two Different PCM Versions and IEF Method[a]

	H_2CO			H_2CNH			HNCO		
	N2	N4	IEF	N2	N4	IEF	N2	N4	IEF
Q_σ^d(theo)		15.7962			13.8217			19.7452	
Q_M^e(out)		−0.1000			−0.1875			−0.1606	
Δ_σ^N	0.0636		0.0223	0.0746		0.0167	0.0842		0.0311
Δ_σ^e	−0.1627	−0.0643	−0.0310	−0.2611	−0.0779	−0.0363	−0.2418	−0.0858	−0.0463
ΔG_{el}	−5.61	−5.76	−5.64	−4.16	−4.74	−4.54	−6.88	−7.06	−6.90
CPU time	34.5	59.8	49.3	56.2	89.7	79.2	56.9	96.9	83.1

[a] See text for definitions. Charges are in au, energies in kcal/mol, and times in seconds.

the N4 version of PCM the errors on $\mathbf{q}^N$ charges are corrected exactly in the same way as in N2, whereas the effects due to the solute escaped charge, Q_M^e(out), are taken into account in a more refined way.

The escaped electronic charge is calculated exactly on the basis of the flux of the solute electric field through the cavity surface Σ:

$$Q_M^e(\text{out}) = -\left(N_e + \frac{1}{4\pi}\int_\Sigma E_M^e(s)\cdot n_s \, ds\right) \qquad (33)$$

Being a real charge, it should give of its own a contribution to the solvent reaction field via a bulk apparent charge distribution, $\rho_B(\vec{r}) = -(\epsilon-1)/\epsilon\rho_M^e(\vec{r})$, spreading outside the cavity. In the N4 procedure this contribution is approximated in terms of an additional apparent surface charge distribution σ_{eff} which is treated exactly in the same way as the original one, and discretized in a further set of apparent charge $\{q_{eff}\}$ by exploiting the same tessellation of the cavity surface into tesserae already used in the PCM program.

Going to the IEF method, we can anticipate that the global effect due to all these errors inherent to ASC methods, and in particular that related to the electronic tails outside the cavity, is quantitatively less important (the following numerical results will show the real amount). The reasons for this generalized better behavior can be explained by electrostatic considerations. For example, by assuming a solute radial symmetric electron density, it can be shown that the potential calculated on the related spherical cavity surface is almost by an order of magnitude less sensitive to the escaped charge than the electric field.[16] This "good" behavior of the potential is still osbservable in the general case of a molecular cavity with any charge distribution in it; thus, as IEF exploits both potential-type and electric field-type operators (see eqs 9−11), while PCM only the latter ones; the error on the apparent charges given by IEF will be smaller than the PCM analog. Practically, this means that in IEF calculations, at least on "standard" neutral solutes, these errors can be safely neglected without affecting the final results in a quantitative way.

What reported above has to be kept in mind in order to better understand the following numerical analysis focussed on some comparative tests between IEF results, computed without any correction of the charges, and those obtained with the two versions of PCM exploiting the two described processes of normalization.

4. Numerical Results

The present section, devoted to report some numerical results obtained within the new IEF formalism, will be divided in three subsections, each one addressed to a specific solute−solvent system. Thus, in the first part we shall analyze some potentialities of IEF in treating standard isotropic solvents, in the second we shall consider a specific application to anisotropic dielectrics, and finally, in the third we shall show some results on ionic solutions. The relative importance given to each section, and the by far longer analysis devoted to the isotropic case, has been led by the methodological character of the present paper, in which the main purpose is to state the validity of the new method, and to show, at least with brief examples, all its great potentialities and not to report detailed applications to specific chemical systems. The latter type of analysis will be reported in future papers each one addressed to a specific solute−solvent system.

All the numerical results reported in the following subsections have been obtained by using the computational package GAMESS.[14]

4.1. Isotropic Dielectrics. For the preliminary isotropic tests we have examined a set of three dipolar solutes (H_2CO, H_2CNH, HNCO) in a dielectric model mimicking water ($\epsilon = 78.5$), using for all of them a DZP plus diffuse functions basis set. The diffuse functions are of dsp-type for heavy atoms and of sp-type for hydrogen, their exponents are $^1/_3$ of the smallest exponents of the corresponding DZP functions.

The comparisons reported in the Tables 1 and 2 will be focussed on two fundamental aspects related to the occurrence of quantitative errors in the apparent charges in the IEF method and in two version of PCM (i.e. N2-PCM, N4-PCM) exploiting the two different normalization procedures described in the section before. In Table 1, we shall report the effects these errors have on the energetic quantities (i.e., on the electrostatic contribution to the solvation free energy, ΔG_{el}) while, in Table 2, we shall quantify the parallel effects on the solute wave function in terms of some molecular electric response functions, e.g dipole moment, static polarizability, and hyperpolarizability tensors.

As an additional technical comparison, in Table 1 we also report the computational times of each method.

About data reported in Table 1, first we have to note the intermediate performances of IEF in terms of time consume. As already said in the previous section, this is due to the fact that IEF method requires the calculation of 4 + 2 matrices (4 of $\mathbf{D}_x/\mathbf{S}_x$ type plus the two solute dependent, $\mathbf{E}_n$ and $\mathbf{V}$), while PCM only 1 + 1 matrices (i.e., $\mathbf{D}$ and $\mathbf{E}_n$); in particular the ratio between IEF CPU times and those obtained in the standard N2-PCM version is of the order of 1.4. However, when we pass to consider the more refined N4-PCM version, the same ratio IEF/PCM is inverted and the PCM times become by far longer; this behavior is easily explained by observing that N4-PCM, besides the standard PCM quantities, has to calculate the escaped charge by a many-point numerical evaluation of the surface integral of eq 33 and to compute the additional set of "effective" charges.

Passing to the problem of the errors, it is worth stressing the higher quality of the approximation used to calculate the total nuclear apparent charge in the IEF method (for PCM we report a single value as both N2 and N4 versions give the same

TABLE 2: Dipole Moment (in debye) and Static (Hyper)polarizability (in au) Data for H_2CO, H_2CNH, and HNCO Obtained with Two different PCM Versions and IEF Method. Values in Parentheses Refer to $(2n + 1)$ Calculations

	H_2CO			H_2CNH			HNCO		
	N2	N4	IEF3	N2	N4	IEF3	N2	N4	IEF
μ_z	−3.6258	−3.6437	−3.6278	−1.3593	−1.3037	−1.3150	−3.6518	−3.4976	−3.4618
α_{xx}	17.7	17.7	18.3	24.2	25.3	25.1	18.0	18.6	18.5
α_{zz}	24.8	25.5	25.6	39.7	42.2	42.3	48.1	51.1	51.2
β_{xxx}	36	38	43	−11	−14	−16	22	26	25
	(40)		(43)	(−14)		(−16)	(23)		(25)
β_{zzz}	47	50	52	122	156	153	176	244	237
	(46)		(52)	(128)		(153)	(197)		(237)
γ_{xxzz}	1277		1617	1147		1485	615		787
	(1400)		(1615)	(1280)		(1483)	(673)		(787)
γ_{xxxx}	1734		2152	2243		2886	895		1073
	(1893)		(2149)	(2550)		(2882)	(988)		(1072)
γ_{zzzz}	1102		1447	2675		4220	3853		6395
	(1273)		(1444)	(3412)		(4207)	(4935)		(6378)

unrenormalized charge): the differences with respect to the Gauss theorem value are always of the order of 0.15%, while for PCM they oscillate around 0.4−0.6%. This behavior can be safely taken as the definitive proof of the good reliability of the integration techniques used in the evaluation of **C** and **g** matrices.

A different analysis is needed to explain the much larger differences obtained in the three methods for the total electronic apparent charge. Here, the quite diffuse basis set exploited gives rise to a not negligible fraction of escaped charge (its exact value ranges from about 0.1 to 0.2 unit charge) and thus to tail-induced errors. The immediate consequence is that the final error on $Q_\sigma^e(\text{comp})$ is larger than on $Q_\sigma^N(\text{comp})$ in all the methods, even if by quite different quantities. IEF computed values differ from the theoretical analogs of quantities of the order of 0.2%, while for PCM we obtain differences reaching 1.9% in the N2 version, and 0.6% in N4 version. We recall that, as mentioned in the previous section, in the N4 version the computed electronic charge is given by the sum of two sets of apparent charges (i.e., standard and effective), and, as a result, the remaining error is due to the discretization only, exactly as in the case of the nuclear counterpart (in other words, for N4 we always have $|\Delta_\sigma^N| \approx |\Delta_\sigma^e|$).

The analysis above has been reported in many such details as it gives useful hints to understand the final effects on both the electrostatic solvation free energy of Table 1 and the molecular electric properties reported in Table 2.

What we can say about ΔG_{el} values is only a partial analysis as other contributions, of nonelectrostatic origin, should be considered in order to do a reliable comparison with experimental measurements; anyway, for our purposes, it is enough to limit such comparison to an internal analysis and derive the good quality of IEF results from their large similarity with those obtained with the N4 version of PCM, which in many previous calculations has shown a by far more reliable behavior than N2-PCM. We stress that this good agreement between IEF and N4-PCM is a very important point as IEF results are obtained without any correction for the charge errors, while the N4-PCM, as already said, exploits a very refined procedure to take into account the tail charge effects.

Indeed, the IEF method when supplemented with the specific techniques implemented to get nonelectrostatic contributions has given very good results in high agreement with experimental data; for molecular solutes similar to those presented here, the mean error found is always below 0.3 kcal/mol.

Actually, the variations of the free energy from one method to the other are very small, the latter in fact is well-known to be a not very sensitive quantity; by far larger changes can be observed in the calculation of the electric response functions.

The specificity of these calculations derives from different sources; first, in order to get good results one has to use very large basis sets, including a sizable number of diffuse functions, hence the solute charge distribution is more likely spread in a larger volume. In addition one has to compute first, second, and third derivatives of this charge with respect to an external field.

In the recent PCM implementation of the algorithm for the analytical computation of (hyper)polarizabilities, the evaluation of such derivatives is obtained by resorting to the CPHF formalism.[19,20] In this framework it can be shown that the effects of charge tails, which in the zero-order calculation can be taken into account through the normalization procedures indicated above without affecting the results too much, at higher orders are largely amplified. This amplification may become so important to prevent PCM procedure to exploit a simplified computational technique, known as $(2n + 1)$ scheme, which should imply improved accuracy (iterative solutions of the CPHF equations are generally not exact), less computational time demands, and memory savings. In brief, the $(2n + 1)$ rule states that knowledge of the wave function through order n allows one to calculate the energy through order $(2n + 1)$; passing to the energy derivatives, this means that for both the first and second hyperpolarizabilities the order of the required wave function derivatives is lower by 1 compared to the standard iterative scheme. In the standard PCM framework the formal derivation of this scheme is no more valid because of numerical reasons. Roughly, this can be explained by recalling that the error one makes in the computation of the electronic charges at a given order of perturbation is different from that obtained in the immediately lower-order calculation because of the different magnitude of the "differential charge tails" at various orders and the high sensitivity of PCM to them.

In Table 2 we report the major components of the dipole moment and a selection of static (hyper)polarizability tensor components for the same molecules as obtained with the three procedures exploited above. Dipole values are in debyes, whereas all (hyper)polarizabilities are in au; results in parentheses refer to $(2n + 1)$ calculations. For N4-PCM this technique is not implemented as well as the evaluation of the second hyperpolarizability. The molecular solutes, all planar, are placed on the xz plane with the major axis along z.

The most evident characteristic resulting from the data of Table 2 is that, for IEF, analytical and $(2n + 1)$ derived hyperpolarizability values are almost equal (the percentage error is almost 0 for β, and always smaller than 0.3% for γ). On the contrary, for N4-PCM the same errors ranges between 10 and 30% for both β and γ. Moreover, it is worth remarking that, as for free energy values, also the electric response functions,

TABLE 3: Electrostatic Free Energy Values of the Single Reactants, Their Sum (R), and the TS with Respect to the Dielectric Anisotropy[a]

	$\Delta\epsilon = 10.00$	$\Delta\epsilon = 19.44$	$\Delta\epsilon = 38.67$	$\Delta\epsilon = 57.50$
Cl^-	−0.22	−0.54	−1.10	−1.48
CH_3Cl	−0.07(+0.01)	−0.13(0.00)	−0.20(−0.03)	−0.25(−0.05)
R	−0.19(−0.11)	−0.57(−0.44)	−1.20(−1.03)	−1.63(−1.43)
TS	−0.17(−0.17)	−0.30(−0.44)	−0.32(−1.00)	−1.01(−1.52)

[a] Energies (in kcal/mol) are calculated with respect to the corresponding values obtained with $\Delta\epsilon = 0$.

i.e., μ, α, and β, calculated with IEF methods are very similar to those obtained with N4-PCM, which, on the contrary, can be very different from the parallel N2-PCM values (the difference being larger for β).

Both these analysis, either on the free energy or on molecular properties, can be safely taken as proofs, on the one hand, of the reliability of the IEF method, and on the other hand, of its high numerical quality which, at least in the specific cases analyzed above, is even better than that of other ASC methods.

The high quality shown for isotropic dielectrics has been analyzed in such detail as will be important to state the reliability of results reported below for the two other systems, namely anisotropic dielectrics and ionic solutions, for which we cannot exploit simple checks as that given by the Gauss law for isotropic solvents.

4.2. Anisotropic Dielectrics. It has been found that thermotropic liquid crystals for which mesomorphic properties are maintained over a wide temperature range have high potential as unique reaction solvents, because their rigidity of molecular ordering and fluidity make them suitable for solute diffusion.[21] The ability of liquid crystal phases to control reactivity is recognized to depend on a number of factors, including the shape of the reactant molecules, flexibility, polarizability, and mesophase type of the medium.

Using this experimental results as a hypothesis, we have tried to apply IEF to the study of the S_N2 symmetric reaction between Cl^- and CH_3Cl in an anisotropic dielectric mimicking a nematic phase of positive anisotropy; in our framework of a continuum solvent, this means to define a diagonal dielectric tensor ϵ whose principal values represent the value of the permittivity along and perpendicular to the solvent ordering axis, namely $\epsilon_{||}$ and $\epsilon_{\perp}$, with $\Delta\epsilon = \epsilon_{||} - \epsilon_{\perp} > 0$. In particular, we can choose the reference coordinate frame such that $\epsilon_x = \epsilon_y = \epsilon_{\perp}$, and $\epsilon_x = \epsilon_{||}$.

As our purpose was to check the performances of our method, we have not considered a real anisotropic dielectric, but we have defined five hypothetical nematic phases with a dielectric anisotropy, $\Delta\epsilon$, ranging from 0 to ∼58, where 0 indicates the limit isotropic case with $\epsilon_{||} = \epsilon_{\perp}$. These systems have been defined in such a way as that all have the same value of the geometrical average permittivity, $\epsilon_M = (\epsilon_{\perp}^2\epsilon_{||})^{1/3} = 7.21$; the latter value has been chosen starting from an anisotropic system with a dielectric tensor recalling those of the most used real liquid crystals, namely $\epsilon_{\perp} = 5$, $\epsilon_{||} = 15$, and $\Delta\epsilon = 10$.

The data reported in Table 3 refer to the electrostatic free energy values (in kcal/mol) of the single reactants, their sum (indicated as *R*), and the transition state (TS), obtained at geometries optimized in vacuo and with a standard 6-311G** basis set. The two values given for CH_3Cl, R, and TS at each $\Delta\epsilon \neq 0$ refer to calculations done with the molecule major axis along and perpendicular to *z* axis, respectively. All data are relative to the $\Delta\epsilon = 0$ value.

In Figure 1 we report the trend of the electrostatic contribution to the activation free energy $\Delta G^{\ddagger}_{el}$ with respect to the dielectric anisotropy, $\Delta\epsilon$. The two plotted curves refer to two hypothetical reaction paths, obtained by supposing that both the reactants and the resulting TS are oriented along and perpendicular to the *z* axis, respectively.

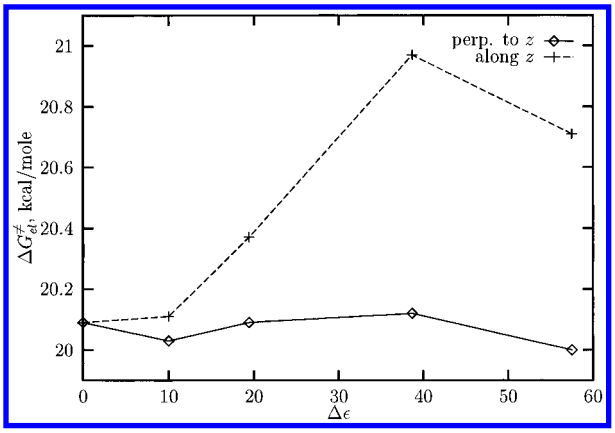

Figure 1. Electrostatic contribution to the activation free energy of the $Cl^- + CH_3Cl$ reaction, with respect to the dielectric anisotropy. The two curves refer to the two hypothetical reaction paths described in the text. Energies are in kcal/mol.

A first analysis of both Table 3 and Figure 1 leads to recognize some interesting trends. On the one hand, we can note that the nonnegligible effect of the dielectric anisotropy on the free energy value of the reactants CH_3Cl and of the TS is opposite; the first is better stabilized in the "along z" orientation, while the second is almost insensitive to the orientation for the first two $\Delta\epsilon$ values, while at very high anisotropy the perpendicular orientation becomes the most favored; clearly for the spherically symmetric case of Cl^- we cannot define two different orientations.

The explanation of these behaviors is not easy; what we can suppose to happen is that the dipolar CH_3Cl affects a higher solvent stabilization when its dipole is parallel to the solvent orientation axis along which the permittivity value is larger, because, in this case, the solute−solvent interactions are almost of dipole−dipole nature; on the contrary, for the symmetric and nonpolar $ClCH_3Cl$−TS the same interactions have a different origin, and maybe higher-order moments having opposite trends become important. Anyway, whatever are the causes of these free energy behaviors, the final effect we observe is a not linear trend on the related activation energy values which show a maximum at $\Delta\epsilon = 38.7$ for the along *z* reaction path, and a minimum at $\Delta\epsilon = 10$ for the other one.

As we have already noted, the analysis above is limited to the electrostatic effects only; actually another contribution to solute−solvent interactions, i.e., that related to steric factors, should be taken into account in order to give a more reliable explanation of data; the latter contribution, usually indicated as cavitation, seems in fact to be very important, in some cases even more effective than the electronic one, in the ability of liquid crystal packing arrangements to lead to preferential solute orientations and, indirectly, reaction pathways. In particular, it has been experimentally found that the anisotropic rigidity of the local solvent order plays an important role in controlling the stereochemical course of bimolecular reactions, resulting in a high level of diastereoselection.[22]

Indeed, the steric contribution can be evaluated, within the IEF framework, by applying a modified version of the hard particle theory, as given in ref 23. This procedure, which was originally evaluated for a previous computational procedure implemented in the PCM framework to treat the anisotropic systems via a combined BEM/FEM technique (there, ASC charges coming from BEM were supplemented by volume point charges given by FEM, and both sets were then used to define

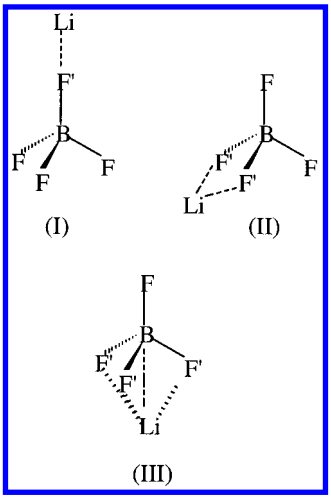

Figure 2. Modes of coordination for $BF_4^-Li^+$ ion pair: I, monodentate (C_{3v}); II, bidentate (C_{2v}); III, tridentate (C_{2v}).

TABLE 4: Optimized Geometries (Å) and Energies (au) for $LiBF_4$ Ion Pair Structure at the 6-311G Level in Vacuo. Values in Parentheses Refer to Calculations in Water**

	structure I	structure II	structure III
energy	−430.29119	−430.31791	−430.31304
	(−430.38337)	(−430.38663)	(−430.37428)
LiB	3.19(3.38)	2.34(2.60)	2.08(2.45)
LiF′	1.62	1.77	1.94
BF	1.35	1.34	1.32
BF′	1.56	1.46	1.42
LiBF′	0.0	49.2	64.1
FBF′	114.5	110.0	115.9

$\hat{V}_R$ and to get the electrostatic contribution to the solvation free energy[24]), is now included into IEF computational code.

Anyway, this further contribution of steric nature is not reported here as it is beyond the purposes of the present paper; a much more detailed analysis of this and other similar reactions, in which both the contributions are taken into account, will be given in a future paper.

4.3. Ionic Solutions. As a last application of IEF formalism let us now consider the problem of solutes immersed in solutions with non zero ionic strength. This problem of very large importance in biomolecular studies is here analyzed from a quite different point of view.

In the following we shall report some results of a theoretical study on the structural consequences of ion pairing when a solvent, without and with mobile salt ions dissolved in it, is taken into account. In particular, we shall present data obtained for the ion pair of BF_4^- with the cation Li^+ in water at 0 and 1 M ionic strength.

The gas phase structure of this molecule has been the object of several studies.[25−27] $LiBF_4$ is a polytopic molecule, in which Li can shift along a surface surrounding BF_4. Three relevant structures with different coordination of the metal have been found experimentally and confirmed by ab initio calculations in vacuo: a monodentate structure I with C_{3v} symmetry, a bidentate C_{2v} structure II, and a tridentate C_{3v} structure III (the three structures are reported in Figure 2). The in vacuo order of stability has been shown to be II > III > I at all levels of calculations.

The same problem must be considered again when the solvent interaction term is introduced in the Hamiltonian. The Li−BF_4 polytopic bond has a noticeable ionic character which could be remarkably affected by solvent interactions, and a fortiori by the presence of mobile salt concentrations. In addition, one should carefully investigate whether the solvent induces heterolytic scission of the complex into separate ions connected by solvent molecules.

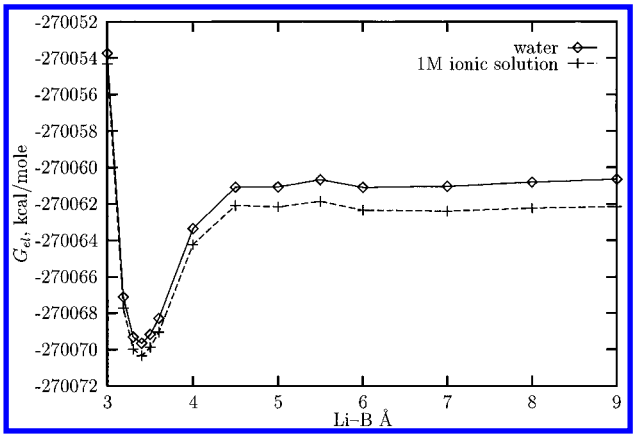

Figure 3. Electrostatic free energy curve with respect to the Li−B distance (in Å) for the $LiBF_4$ structure I. Solid line refers to calculations in pure water, while the interrupted line to calculations in 1 M ionic solution.

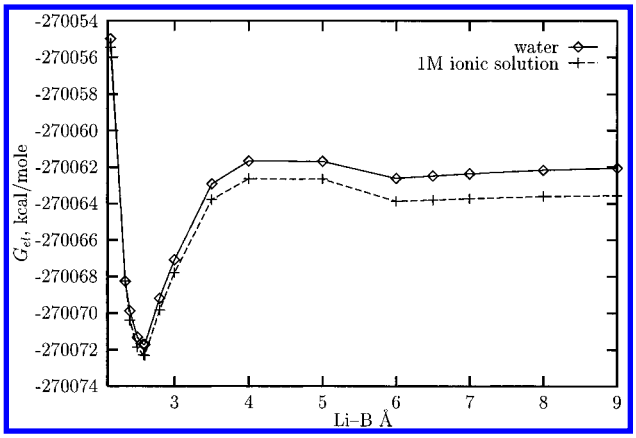

Figure 4. Electrostatic free energy curve with respect to the Li−B distance (in Å) for the $LiBF_4$ structure II. Solid line refers to calculations in pure water, while the interrupted line to calculations in 1 M ionic solution.

To check on these questions we performed some calculations with a 6-311G** basis set varying the Li−B distance but keeping the internal geometry of the BF_4 fragment fixed at the value optimized in vacuo. It has been shown that such a constraint does not alter the relative energy of the three structures too much.

The most significant informations emerging from these calculations are summarized in Table 4 and Figures 3−5. In Table 4 we report the fully optimized geometries and energies for the three structures in vacuo and the related optimized Li−B distances and energies in water.

From data reported in Table 4 we can first note that the relative ordering of the energy at the minima is changed passing from vacuum to water; the role of structures I and III is reversed, and the final order becomes II > I > III. In addition, all the condensed phase minima are displaced toward larger Li−B distances with respect to the vacuum values. In Table 4 we have not reported the results for the ionic solution as the optimized Li−B distances remain completely unchanged with respect to the pure water values; the only observed changes are in the shift of all the corresponding free energies toward more negative values.

The latter effect of stabilization of the $LiBF_4$ ion pair when a salt concentration is added to the solvent is better visualized in Figures 3−5, in which we report the electrostatic free energy

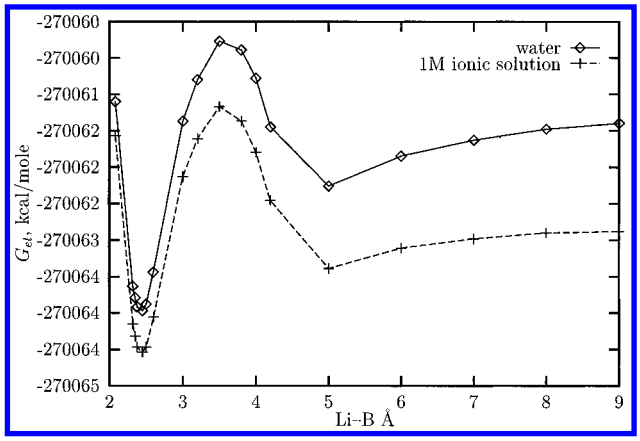

Figure 5. Electrostatic free energy curve with respect to the Li−B distance (in Å) for the $LiBF_4$ structure III. Solid line refers to calculations in pure water, while the interrupted line to calculations in 1 M ionic solution.

curves with respect to the Li−B distance obtained for each structure in pure water and in the ionic solution.

All the three figures show an evident common characteristic: for each structure the two curves are equivalent in shape while the difference between the two energies of each point becomes larger as the Li−B distance is progressively increased (the computed range is 0.4−1.5 kcal/mol for all the structures).

The same curves should also show another interesting aspect, this time not specifically due to the ionic strength, but more generally to the solvent effect: namely, the eventual appearance of a relative minimum at large Li−B distance due to the formation of a solvent-separated ion pair in which the linking bridge is given by a solvent molecule placed exactly between Li^+ and BF_4^-. Actually, this analysis is quite difficult to perform because of the procedure we exploit to build the molecular cavity along the whole path. In the following we report a brief digression which will try to explain this point.

In general, one may define different kinds of molecular surfaces, depending on the specific solute-solvent interactions one wants to take into account. In particular, in order to evaluate the electrostatic term, the only considered here, a solvent excluding surface should be exploited. The latter can be defined as the contact surface of a probe sphere (with radius equal to the molecular radius of the solvent molecules) rolling on the van der Waals surface. The GEPOL computational technique used in IEF to define the molecular cavity and the tessellation of its surface into tesserae describes solvent-excluding cavities in terms of spheres centered on solute atoms, to which some additional spheres are eventually, added. The latter are created with a sequential algorithm: when two spheres of the original cavity are close enough to exclude the solvent from the space between them, one or two additional spheres, not centered on atoms, are added, and the procedure is repeated to a prefixed threshold, considering each time all the possible couples of spheres, both of the first and the following generations.

In the present context of the Li atom, going progressively far away from the fixed BF_4, the definition of the proper cavity becomes more and more complex, as the number of spheres to be added increases until a value at which the cavity is separated in two distinct cavities containing Li^+ and BF_4^-, respectively. This point is clearly a source of an abrupt change, as it leads to a suddenly greater solvent effect with respect to the immediately preceding points, all characterized by a single cavity. This can be reflected in the corresponding free energy curve in terms of an unphysical jump, which makes the identification of the searched relative minimum quite difficult.

Here, we limit ourselves to point out the problem, without giving any recipe to overcome it, as this would imply to go far beyond the scope of the present section; a more detailed analysis is now under study.

5. Conclusions

In this paper we have addressed our attention to the electrostatic interaction between a molecule and its environment, showing that integral equation formulations are still efficient in the extension of continuum solvation methods to both solvent with intrinsic dielectric anisotropy, like liquid crystals but also solid matrices, and ionic solution.

To this end, we have presented two preliminary applications, i.e., a simple S_N2 reaction in an isotropic solvent and an ion pairing in a solution with not zero ionic strength, which should give a first view on the interesting research fields opened by the possibility of treating these nonstandard solute−solvent systems with a method much more efficient than the 3D methods, namely finite difference and/or finite element, used so far.

The computational method presented here is readily adaptable to current programs for the calculation of molecular wave functions and properties; as a first example of these potentialities, we have shown that IEF method can be usefully exploited to obtain reliable values of the static (hyper)polarizabilities, both through standard iterative and $(2n + 1)$ schemes. The latter application also shows that IEF is by far less affected by both the numerical and physical errors on the apparent charges than standard PCM; this aspect, if associated to the new general applicability of IEF to molecular solutes of any shapes, leads to definitely include IEF among the most effective methods also for standard isotropic dielectrics. Actually, as IEF, contrary to all the other QM continuum methods, manages to treat very different solute−solvent systems with almost the same computational expense and the same reliability in the results, we may certainly consider it as one of the most promising solvation models, even if the still poor number of checking tests performed until now must lead to a cautionary attitude.

Acknowledgment. The authors acknowledge the Consiglio Nazionale delle Ricerche (CNR) for financial support.

References and Notes

(1) Beveridge, D. L., Jorgensen, W. L., Eds. *Computer Simulations of Chemical and Biochemical Systems*, N.Y. Academy of Science: New York, 1986.
(2) Allen, M.; Tildesley, D. J. *Computer Simulation of Liquids*, Clarendon: Oxford, UK, 1987.
(3) Tomasi, J.; Persico, M. *Chem. Rev.* **1994**, *94*, 2027.
(4) Cancès, E.; Mennucci, B. *J. Math. Chem.*, submitted for publication.
(5) Cancès, E.; Mennucci, B.; Tomasi, J. *J. Chem. Phys.* **1997**, *107*, 3032.
(6) Yomosa, S. *J. Phys. Soc. Jpn.* **1974**, *36*, 1655.
(7) Harned, H. S.; Owen, B. B. *The physical Chemistry of Electrolytic Solutions*, Reinhold Publ. Corp.: New York, 1950.
(8) Hackbusch, W. *Integral Equations-Theory and Numerical Treatment*; Birkhäuser Verlag: Basel, Switzerland, 1995.
(9) Miertuš, S.; Scrocco, E.; Tomasi, J. *Chem. Phys.* **1981**, *55*, 117.
(10) Cammi, R.; Tomasi, J. *J. Comput. Chem.* **1995**, *16*, 1449.
(11) Barone, V.; Cossi, M. *J. Phys. Chem.*, submitted for publication.
(12) Klamt, A.; Schüürmann, G. *J. Chem. Soc., Perkin Trans.* **1993**, *2*, 799.
(13) Pascual-Ahuir, J. L.; Silla, E.; Tomasi, J.; Bonaccorsi, R. *J. Comput. Chem* **1987**, *8*, 778.
(14) Schmidt, M. W.; Baldridge, K. K.; Boatz, J. A.; Elbert, S. T.; Gordon, M. S.; Jensen, J. H.; Koseki, S.; Matsunaga, N.; Nguyen, K. A.; Su, S. J.; Windus, T. L.; Dupuis, M.; Montgomery, J. A. *J. Comput. Chem.* **1993**, *14*, 1347.
(15) Chipman, D. M. *J. Chem. Phys.* **1997**, *106*, 10194.
(16) Klamt, A.; Jonas, V. *J. Chem. Phys.* **1996**, *105*, 9972.
(17) Cossi, M.; Mennucci, B.; Pitarch, J.; Tomasi, J. *J. Comput. Chem.*, submitted for publication.
(18) Mennucci, B.; Tomasi, J. *J. Chem. Phys.* **1997**, *106*, 5151.

(19) Cammi, R.; Cossi, M.; Tomasi, J. *J. Chem. Phys.* **1996**, *104*, 4611.
(20) Cammi, R.; Cossi, M.; Mennucci, B.; Tomasi, J. *J. Chem. Phys.* **1996**, *105*, 10556.
(21) For recent reviews, see: (a) Ramamurthy, V. *Tetrahedron* **1986**, *42*, 5753. (b) Scheffer, J. *Tetrahedron* **1987**, *43*, 7. (c) Kreysig, D.; Stumpe, J. In *Selected Topics in Liquid Crystal Research*; Koswing, H. D., Ed.; Akademine-Verlag: Berlin, 1990; Chapter 4. (d) Leigh, W. J. In *Liquid Crystals. Applications and Uses*; Bahadur, B., Ed.; World Scientific: Singapore, 1991; Chapter 27. (e) Weiss, R. G. In *Photochemistry in Organized and Constrained Media*; Ramamurthy, V. Ed.; VCH Publishers: New York, 1991; Chapter 14.
(22) Kansui, H.; Hiraoka, S.; Kunieda, T. *J. Am. Chem. Soc.* **1996**, *118*, 5346.
(23) Mennucci, B.; Cossi, M.; Tomasi, J. *J. Phys. Chem.* **1996**, *100*, 1807.
(24) Mennucci, B.; Cossi, M.; Tomasi, J. *J. Chem. Phys.* **1995**, *102*, 6837.
(25) Zakzhevskii, V. G.; Boldyrev, A. I.; Charkin, O. P. *Chem. Phys. Lett.* **1980**, *73*, 54.
(26) Loewenschuss, A.; Marcus, Y. *Chem. Rev.* **1984**, *84*, 89.
(27) Francisco, J. S.; Williams, I. H. *J. Phys. Chem.* **1990**, *94*, 8522.